Molecular BioSystems

PAPER

View Article Online
View Journal

Cite this: DOI: 10.1039/c4mb00703d

Reversible redox modifications in the microglial proteome challenged by beta amyloid†‡

Virginia Correani,[a] Laura Di Francesco,[a] Isabella Cera,§[a] Giuseppina Mignogna,[a] Alessandra Giorgi,[a] Michele Mazzanti,[b] Lorenzo Fumagalli,[c] Cinzia Fabrizi,[c] Bruno Maras[a] and M. Eugenia Schininà*[a]

Microglia are resident macrophages in the central nervous system, whose participation against exogenous injuries and infections is mainly marked by an immediate release of inflammatory cytokines along with a toxic efflux of superoxide radicals. Indeed, many lines of evidence indicate that persistent activation of these cells turns their neuroprotective phenotype into a neurotoxic one, which contributes to destroy neuronal activity and induces neuronal loss in several neurodegeneration processes, such as Alzheimer's disease. In this study we attempted to fill-in the gap in our knowledge about redox regulation of amyloid activated microglia. With this aim, we carried out a robust and comprehensive characterization of the reversibly redox modified proteome both at the level of resting and amyloid-activated BV2 cells, an immortalised cell line of murine microglia. The approach we used combined the selective enrichment of reversible redox modified proteins through a biotin bait with nanoscale liquid chromatography tandem mass spectrometry of their proteolytic peptides. By this reliable approach, we identified 60 proteins changing the redox status of their selective cysteine residues upon treatment with the amyloidogenic $A\beta_{25-35}$ peptide. These results assessed that in microglia stimulated by amyloids, redox modifications of the proteome specifically target proteins involved in crucial cell processes, *i.e.* those involved in the protein synthesis. In particular, for peroxiredoxin-6 (Prdx6) and Ras-related C3 botulinum toxin substrate 1 (Rac1) we suggest mechanisms through which reversible redox modifications could affect the peculiar role of microglia in amyloidogenic injury, which at the same time reinforce the oxidative burst and resist toward it. Moreover, the redox modulation we observed on chloride intracellular channel protein 1 (CLIC1) strengthens the structural and functional relationship between the oxidative stress and the metamorphic transition of this protein from a soluble form to an integral membrane form. The redox signatures we determined might also provide neurologists with more specific and reliable biomarkers to distinguish the diverse microglia status in neurodegeneration and then to drive targeted drug design.

Received 10th December 2014,
Accepted 17th February 2015

DOI: 10.1039/c4mb00703d

www.rsc.org/molecularbiosystems

Introduction

Alzheimer's disease (AD) is an age-related neurodegenerative disorder characterized by a progressive loss of neurons and synapses, mostly in the cerebral cortex.[1] In AD, molecular hallmarks of neuronal damage are both intracellular aggregates of the hyperphosphorylated Tau protein and extracellular insoluble fibres made up of beta-amyloid (Aβ) peptides, released by the sequential cleavage of the membrane Amyloid Precursor Protein (APP) by beta and gamma secretases.[2] However, only the Aβ soluble oligomer precursors of the insoluble fibres have been proved to be neurotoxic, and therefore regarded as the main aetiological agent in AD neurodegeneration.[3] Although the precise mechanisms by which Aβ peptides trigger neurodegeneration remain unclear, one of the established biochemical features of AD injured tissues is an unbalanced cellular redox state, mainly triggered in the glial compartment.[4,5]

Microglia are resident macrophages of the central nervous system that play an essential role in homeostasis maintenance, tissue repair, innate immunity response and neuroinflammation.[6] In response to injuries and infections these cells are able to release inflammatory cytokines along with the toxic efflux of

[a] *Dipartimento di Scienze Biochimiche, Sapienza University of Rome, Piazzale Aldo Moro, 5, 00185 Rome, Italy. E-mail: eugenia.schinina@uniroma1.it; Fax: +39 06 4440062; Tel: +39 06 49910605*
[b] *Dipartimento di Bioscienze, Università degli Studi di Milano, Milan, Italy*
[c] *Dipartimento di Scienze Anatomiche, Istologiche, Medico-Legali e dell'Apparato Locomotore, Sapienza University of Rome, Rome, Italy*

† This paper is dedicated to the memory of our beloved colleague, Prof. Donatella Barra, for his unforgettable guidance in science and life.

‡ Electronic supplementary information (ESI) available. See DOI: 10.1039/c4mb00703d

§ Current address: Institute for Neuroscience, Medical University of Innsbruck, Innsbruck, Austria.

superoxide radicals produced by the NADPH oxidase complex.[7] Although upon this oxidative burst the extracellular environment becomes strongly oxidative, the microglia themselves are able to proliferate and differentiate. Therefore, microglia should be considered as cells intrinsically resistant to oxidative stress.

However activated microglia do not constitute a unique cell population.[8,9] Upon any homeostatic disturbance that may challenge the neuronal compartment (ranging from cell debris to diverse toxins), quiescent microglia, in a tight cross-talk with neurons and astrocytes, are known to assume a diversity of reactive states to alternatively prime debris clearance, tissue repair or neuronal death.[10] With the aim of discovering therapeutic agents selectively targeting the neurotoxic state(s), nowadays much effort has been put into identifying biomarkers which can distinguish different microglia states.[11,12] The neurotoxic state of microglia in AD is reasonably pushed by the oxidative stress and thus studies dedicated to identify changes in the proteome redox states may help in designing targeted therapies.

Protein cysteinyl residues are among the possible sensitive sites of an altered concentration of redox metabolites. Although cysteine is one of the least abundant amino acids in the proteome, this residue often plays a pivotal role in the fragile equilibrium between protein folding and misfolding. When under oxidative stress the intracellular environment switches from a reductive state to an oxidative state, cysteines at the protein surface may stochastically form intermolecular disulfide bridges, leading to intracellular proteinaceous polymers which in turn may impair cell functions. In this scenario, any post-translational modification of cysteinyl residues may play a key role in protecting intracellular proteins from these irreversible modifications.[13] Nonetheless, recent evidence shows that reversible post-translational modification of cysteines, like the covalent binding of glutathione (GSH) by *S*-glutathionylation and of the nitric oxide ($^{\bullet}$NO) moiety by *S*-nitrosylation, may represent a key step in protein functional regulation and cell signalling.[14,15] Indeed, the presence of enzymes inside the cell with the ability to catalyse protein *trans*-glutathionylation and *trans*-nitrosylation (*e.g.* glutathione *S*-transferases, *S*-nitrosoglutathione reductase, glutaredoxin and thioredoxin systems) suggests that these reversible redox modifications (hereafter RRMs) may give rise to molecular networks similar to that generated by protein phosphorylation/dephosphorylation.[16,17] In turn, the modification of cysteinyl residues by *S*-glutathionylation and *S*-nitrosylation is emerging as a key step in neurodegenerative diseases, as well as in other chronic pathologies like type 2 diabetes and multiple sclerosis.[18–20]

In AD, the knowledge of the role of *S*-glutathionylation and *S*-nitrosylation is only at the beginning level.[21–23] Technical difficulties in ''trapping'' the thiol states of cysteinyl residues into cell lysates and in avoiding disulfide shuffling during proteome manipulations may explain the paucity of the available data. In this study, we investigated in microglia the effects of amyloid peptides on the redox state of the proteome cysteinyl residues, generally referred to as the redox-proteome.[24] For this purpose, we applied on a microglial cell culture upon amyloid treatment a targeted strategy for a proteome-wide identification of cysteinyl residues that undergo reversible oxidation.[25] With the results achieved, we suggest a role for RRMs in triggering microglia towards the activated phenotype responsible for neuroinflammation in AD.

Material and methods

Chemicals and materials

An immortalised murine microglial cell line, BV-2, continuously maintained at the Dipartimento di Scienze Anatomiche, Istologiche, Medico-Legali e dell'Apparato Locomotore, was an original gift of Prof. Giulio Levi (Istituto Superiore di Sanità, Rome). Dulbecco's modified Eagle's medium, fetal calf serum, penicillin, streptomycin and glutamine were obtained from Sigma-Aldrich. The $A\beta_{25-35}$ (GSNKGAIIGLM) peptide was obtained from Bachem (AG, Bubendorf, Switzerland). Ammonium bicarbonate, β-mercaptoethanol, urea, 3-[(3-cholamidopropyl)dimethylammonio]-1-propanesulfonate (CHAPS), sodium chloride, and *N*-ethyl maleimide (NEM) were purchased from Sigma-Aldrich (St. Louis, MO, USA). Ethanol, water, acetonitrile (ACN), and formic acid (FA) were purchased from Fluka Chemie (AG, Buchs, Switzerland). Potassium chloride, dibasic sodium phosphate and monobasic potassium phosphate were purchased from Merck KGaA (Darmstadt, Germany). From Bio-Rad (Hercules, CA, USA) were purchased Tris-HCl, dithiothreitol, Triton X-100 and the Bradford reagent. The protease inhibitor cocktail (Complete, mini Protease inhibitor cocktail tablet) was supplied by Roche (Mannheim, Germany). EZ-link *N*-[6-(biotinamido)hexyl]-3′-(2′-pyridyldithio)propionamide-biotin and high capacity streptavidin-agarose resin were purchased from Thermo-Scientific Pierce (Rockford, IL, USA). Trypsin was purchased from Promega (Madison, WI, USA). C_{18} reverse-phase loaded Empore™ SPE disks were procured from Sigma-Aldrich. Fused silica capillaries were obtained from New Objective (Woburn, MA, USA), and C_{18} reverse-phase beads from Michrom Bioresources (Auburn, CA, USA). All aqueous solutions were prepared using ultrapure water (18.2 MΩ cm^{-1}) from a Milli-Q water purification system (EMD Millipore, Billerica, MA, USA).

Cell cultures

The murine microglial cell line BV2[26] was grown in Dulbecco's modified Eagle's medium (DMEM) supplemented with 100 U ml^{-1} penicillin, 100 μl ml^{-1} streptomycin, 10% fetal calf serum and 2 mM L-glutamine; cultures were maintained at 37 °C in 5% CO_2/95% humidified air atmosphere.

Synthetic $A\beta_{25-35}$ (GSNKGAIIGLM) peptides were dissolved in sterile distilled water at a concentration of 1 mM and incubated for 72 h at 37 °C to allow aggregation.[27]

BV2 cells were cultured in a 75 cm^2 culture flask at a density of 5×10^6 cells per flask, washed with serum-free media, and challenged with 50 μM $A\beta_{25-35}$ peptide for 24 h.

Isolation of reversibly oxidized thiol-containing proteins

Three replicates each for $A\beta_{25-35}$ treated and untreated (control) BV2 cells were harvested, washed twice with phosphate buffer saline (PBS) containing 1.37 M NaCl, 27 mM KCl, 100 mM Na_2HPO_4,

and 18 mM KH_2PO_4, and lysed in an alkylating buffer containing 8 M urea, 100 mM *N*-ethyl maleimide (NEM), 50 mM Tris-HCl pH 8.0, 0.1% Triton X-100 and the required amount of the protease inhibitor cocktail according to the manufacturer's instructions. After incubation under rotation at 4 °C for 30 min, three cycles of sonication/relaxation of 30 s were carried out. The protein concentration of each sample was then measured using the Bradford reagent with bovin serum albumin (BSA) as a standard.

Proteins with a reversible oxidation on cysteinyl residues were selectively isolated from these samples using the ''biotin switch'' approach, as further implemented by McDonagh *et al.*[25] and slightly modified for a better recovery of proteins. In brief, equal aliquots (500 μg of proteins) of each lysate obtained from the three replicates of untreated and $A\beta_{25-35}$ treated BV2 cells were precipitated overnight at −20 °C with nine volumes of cold ethanol, and the protein pellet was collected by centrifugation at 14 000 rpm at 4 °C for 15 min to remove the excess of NEM. Reduction of reversibly oxidised cysteinyl residues was then performed re-dissolving all these pellets in 180 μl of a strongly reducing buffer containing 8 M urea, 4% CHAPS, 50 mM Tris-HCl pH 8.0 and 2 mM ethylenediaminetetraacetic acid (EDTA), adding dithiothreitol (DTT) to a final concentration of 20 mM, and incubating for 45 min on a rotator at room temperature. DTT removal was performed by ethanol-precipitation of the protein fraction. Protein thiols have finally been alkylated with a buffer (200 μl) containing a large excess of *N*-[6-(biotinamido)-hexyl]-3′-(2′-pyridyldithio)propionamide (HPDP)-biotin (0.5 mM) for 45 min on a rotator in the dark. After removal of the unbound HPDP-biotin reagent again by ethanol precipitation, equal aliquots of each protein mixture (200 μg) were proteolysed at 37 °C overnight with 200 μl of a solution of sequencing grade trypsin (1 : 50 E/S, w/w) in 50 mM ammonium bicarbonate containing 0.8 M urea. Proteolysis was stopped by adding 200 μl of the denaturing buffer, free of DTT.

The affinity resin was prepared by washing twice an appropriate quantity of the slurry streptavidin-agarose resin in a binding buffer containing 4 M urea, 2% CHAPS, 25 mM Tris-HCl pH 8.0 and 50 mM NaCl. Aliquots of 40 μl of resin (50% slurry) were then incubated with each tryptic peptide mixture at 4 °C overnight on a rotator. After centrifugation at 5000 rpm, each supernatant containing the unbound peptides was re-incubated with a fresh streptavidin-agarose resin, and pooled with the previous resin fraction. The resin samples obtained were washed stepwise with equal volumes (200 μl) of (a) the binding buffer, (b) a buffer containing 8 M urea, 4% CHAPS, 25 mM Tris-HCl pH 8.0, and 1 mM NaCl (two washes), (c) the same buffer without 1 mM NaCl (two washes), and (d) a buffer containing 5 mM ammonium bicarbonate and 20% acetonitrile (ACN; two washes). Peptides from the insoluble resin were finally released by exchanging the *S*-linked biotin-cysteinyl residues with β-mercaptoethanol cysteinyl adducts upon treatment for 5 min at 56 °C with a buffer (25 μl) containing 5 mM ammonium bicarbonate, 20% ACN, and 5% β-mercaptoethanol. The released peptides were collected by centrifugation at 5000 rpm and supernatants were stored at −80 °C.

With the aim of assessing the possible unspecific interactions, minimal aliquots from all the six cell lysates were pooled, and then challenged with streptavidin-agarose beads under the same conditions used for the affinity isolation of peptides containing reversibly modified cysteines described above.

Protein identification

Each of the six peptide mixtures, three biological replicates from resting and three from $A\beta_{25-35}$ treated BV2, was divided into two equal amounts for technical replica (Fig. 1). All these twelve samples were analysed by nano-liquid chromatography combined with tandem mass spectrometry (LC-MS/MS) on an Ultimate3000 system (Dionex, Sunnyvale, CA, USA) equipped with a splitting cartridge for nanoflow and connected on-line *via* a nanoelectrospray ion source (Thermo-Fisher Scientific, Waltham, Massachusetts, USA) to an LTQ-Orbitrap XL mass spectrometer (Thermo-Fisher Scientific).

The samples were preliminarily desalted using C_{18} reverse-phase loaded Empore™ solid phase extraction (SPE) disks, according to the StageTip protocol,[28] resuspended in 0.1% formic acid (FA) and automatically loaded from the autosampler module of the Ultimate 3000 system onto a 10 cm long silica capillary (360 μm o.d., 75 μm i.d. fused silica with an 8 μm i.d. tip, New Objective, Woburn, MA, USA) handmade, packed with the C_{18} reverse phase resin (Magic C_{18}AQ, 5 μm particles, 200 Å pore size), equilibrated in 95% solvent A (5% ACN, 0.1% FA) and 5% solvent B (80% ACN, 0.1% FA). According to the expected complexity, peptide mixtures were fractioned by elution with a 5–80% gradient of solvent B over 110 min at a 300 nl min^{-1} flow rate obtained by a flow split ratio of 1 : 1000.

As peptides were eluted, they were electrosprayed directly into the mass spectrometer with an electrospray (ESI) voltage of 1.9 kV. Mass spectral (MS) data were acquired in a positive mode on the Orbitrap in a Fourier Transform Ion Cyclotron Resonance Mass Spectrometer (FTMS) in the 300–2000 m/z range with a resolution of 30 000 at m/z = 400, an automatic gain control (AGC) target of 1×10^6 ions, and the maximal injection time of 1000 ms. Tandem mass spectra (MS/MS) were acquired on a linear ion trap quadrupole mass spectrometer (ITMS) in data-dependent mode using the Xcalibur™ software, selecting the five most intense ions with charge states ≥ 2 detected per survey scan by FTMS, through collision-induced dissociation (CID), and analysing the resulting fragments in the linear trap (LTQ). LTQ was calibrated using a calibrating mixture (LTQ ESI Positive Ion Calibration Solution Spectra; Thermo-Fisher Scientific) with the following formulation: caffeine (20 μg ml^{-1}), a peptide with sequence Met-Arg-Phe-Ala (1 μg ml^{-1}) and Ultramark 1621 (0.001%) in an aqueous solution of acetonitrile (50%), methanol (25%) and acetic acid (1%). For MS/MS scanning, the minimum MS signal was set to 500, activation time to 30 ms, target value to 10 000 ions, and injection time to 100 ms. All MS/MS spectra were collected using a normalized collision energy of 35% and an isolation window of 2 Th. To avoid redundant sequencing of the most abundant peptides, dynamic exclusion was enabled with a repeat count of 1, a repeat duration of 30 s, an exclusion list size of 300 and an exclusion duration of 90 s.

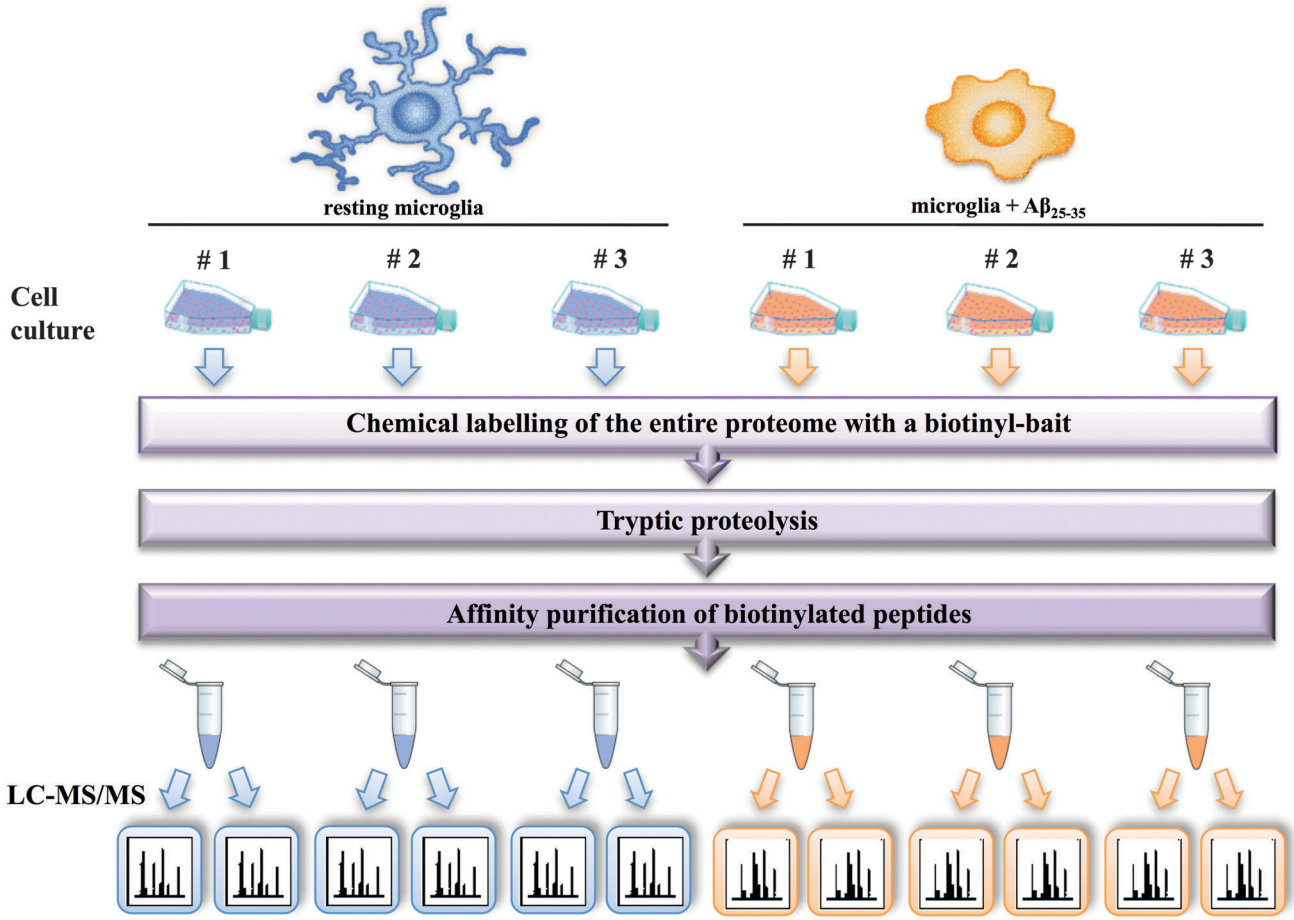

Fig. 1 Workflow of the differential analysis of the reversible redox modified proteome. Reversible redox modified cysteinyl residues of the protein extracts from the BV2 cell line, $A\beta_{25-35}$ treated (microglia + $A\beta_{25-35}$; three biological replicates) and untreated (resting microglia; three biological replicates), were specifically labelled with a biotinyl bait as described in Material and methods. Peptide digests were obtained by trypsin treatment, and biotinyl-labelled peptides were selectively recovered by streptavidin-fishing. Two technical replica derived from each fished mixture were subjected to identification by mass spectrometry. A total of 12 LC-MS/MS experiments were performed. We considered only peptides uniquely assigned to one protein and identified in at least one technical replica of all the three biological replicates of the microglial cultures used.

Data analysis

All mass spectrometric data were analysed using the proteomics software package MaxQuant (version 1.3.5).[29] MS/MS spectra were searched against the *Mus musculus* dataset of UniprotKB database (release 2014_02; 51 373 sequences). Trypsin was selected as the cleavage enzyme. A maximum of two missed cleavages and +4 charge states was allowed for detected peptides. Mass tolerance for FTMS and ITMS measurements was, respectively, set to 20 ppm and 0.5 Da. The false discovery rate (FDR) was set to 0.005 (0.5%) at the protein and peptide levels. The following variable modifications were also used in identification – oxidation of methionine, deamidation of asparagine and glutamine, and reaction of cysteine with mercaptoethanol and NEM. Peptides with a length less than 7 residues were automatically rejected. Matching of 2 min between runs and a minimum ratio count of 1 were set. Searches were also achieved against both a dataset of commonly detected contaminants in proteomics and the reverse decoy database generated by the Andromeda search engine, and the identified peptides were manually removed. Protein identification by only one peptide was manually validated according to Mann *et al.*[30] Moreover, all peptides that were demonstrated (a) to aspecifically interact with streptavidin-agarose beads, (b) not to comprise cysteinyl residues in their sequence, and (c) not to be ascribable either to a protein group unique or to a single gene product, were manually removed from the list. Reversibly redox-modified cysteinyl-containing peptides not identified in at least one technical replica of each of the three biological replicates were rejected.

Assignment of a protein function annotation and clustering of the detected proteins according to molecular and cellular functions were performed using the Ingenuity Pathway Analysis (IPA; www.ingenuity.com). The analysis of enrichment in protein function and cellular processes was based on information contained in the Ingenuity Pathways Knowledge Base. The statistical significance of these enrichments was evaluated by Fisher's exact test.

Total RNA preparation and real-time polymerase chain reaction (RT-PCR)

After the 4 h treatment with $A\beta_{25-35}$, total RNA was purified by 2×10^6 BV2 cells by single extraction with Trizol (Invitrogen) and reverse transcribed by oligo$(dT)_{15-18}$ primers and MML-V reverse trascriptase (Invitrogen). The cDNA was amplified by Taq DNA polymerase in a thermal cycle (PerkinElmer Life Sciences) in the presence of primers for tumor necrosis factor (TNF-α) (5′-primer, GAGCACTGAAAGCATGATCCG; 3′-primer GCAGGTCTACTTTGGGATCATT). The conditions for TNF-α amplification were as follows: 30 s at 94 °C, 30 s at 64 °C, and 30 s at 72 °C. Ten microliters of each PCR product were electrophoresed on 1% agarose gel and then visualized by ethidium bromide staining. The mRNA for glyceraldehyde-3-phosphate dehydrogenase (GAPDH) was used as reference.

Western blot analysis

Protein extracts (approximately, 20 μg) were resolved by 12% sodium dodecyl sulfate (SDS)-polyacrylamide gel electrophoresis (SDS-PAGE; 200 V, 45 min). The protein bands were electrotransferred to nitrocellulose membranes (80 mA, 45 min). Membranes were then treated with a 5% enhanced chemiluminescence (ECL) blocking agent (GE Healthcare Bio-Sciences) in a saline buffer (T-TBS) containing 0.1% Tween-20, 10 mM Tris-HCl, 150 mM NaCl, 1 mM $CaCl_2$, and 1 mM $MgCl_2$, pH 7.4, for 1 h and then incubated with the primary antibody overnight at 4 °C. Subsequently, membranes were washed three times in T-TBS, and the bound antibodies were detected using appropriate horseradish peroxidase-conjugated secondary antibodies, followed by an ECL Plus Western blotting detection system (GE Healthcare Bio-Sciences). ECL was detected using a Molecular Imager® ChemiDoc™ mod. MP System (Bio-Rad Laboratories), and acquired using ImageLab Software, ver. 4.1. Immunodetection was carried out using rabbit polyclonal antibodies (Santa Cruz Biotechnology) against Ras-related C3 botulinum toxin substrate 1 (Rac1; sc-217, dilution 1 : 500), chloride intracellular channel protein 1 (CLIC1; sc-134 859, dilution 1 : 800), peroxiredoxin-6 (Prdx6; sc-134 478, dilution 1 : 200) and against cytokine-inducible nitric oxide synthase (anti-iNOS/NOS-II; Transduction Laboratories 610332, dilution 1 : 10 000) proteins. In each analysed sample, the signal of the target protein was normalized to the corresponding GAPDH (Santa Cruz Biotechnology, sc-32 233; antibody dilution 1 : 500) or β-tubulin (Sigma-Aldrich, T8328; dilution 1 : 10 000) level, which shows comparable expression levels both in treated and untreated cells (Fig. S1, ESI‡). Three replicates were performed, one for each biological sample. All results are expressed as mean ± SD. Differences between experimental groups were determined by Student's *t*-test. The *p*-value of <0.01 was considered statistically significant.

Cell viability

Lactate dehydrogenase (LDH) release into the culture medium was measured using a cytotoxicity detection kit (Roche, Mannheim, Germany) according to the manufacturer's protocol.

Results

With the aim of providing selective targets of oxidative stress in microglia injured by beta amyloid, in this study we approached the identification of reversible redox modified (RRM) cysteinyl residues by mass spectrometry-based proteomics.

Although redox-proteomics is an emerging field in neurobiology, it is a very difficult issue from a methodological point of view. Perhaps the main problem is represented by the requirement to stabilize the proteome thiols against artefactual oxidation.[31] This aim is particularly challenging in 2DE-gel based proteomics, where the high number of sample manipulation steps leads to poorly reproducible assessment of the thiol states of protein spots. To overcome this problem, a significant number of techniques based on resin-assisted enrichment of cysteine-containing proteomes have been proposed (reviewed in ref. 32–34). According to one of these approaches, named ''biotin switch'', immediately after the cell lysis specific RRMs (*e.g. S*-nitrosylation, *S*-glutathionylation, disulfide bridges) are selectively tagged with biotin-derivatives containing a disulfide bridge.[25] The entire proteome was then proteolysed and biotin-containing peptides were selectively isolated by a streptavidin-based affinity step. According to this methodological pipeline, the ''biotin-switch'' has recently provided a reliable evaluation of the redox states of the erythrocyte proteins when coupled with shotgun proteomics.[35]

We applied this approach (schematically summarised in Fig. 1) to BV2 cells, the most frequently used cellular model for microglia in proteomics.[36,37] We treated BV2 with $A\beta_{25-35}$, a shorter and more manageable form of the full-length $A\beta_{1-42}$ peptide, known to be able to induce the inflammatory and oxidative status on microglia, without affecting cell viability (Fig. 2).[11,38–42]

The high degree of selectivity of the ''biotin-switch'' strategy we employed was proved both by the absence of capturing activity against microglial lysates as well as by the high percentage of cysteinyl-containing peptides captured (91%). Moreover, the high yield of the strategy was assessed by the finding in the shotgun proteomics of $A\beta_{25-35}$ treated and untreated cells of a total of 1129 peptides. This number of peptides is in good agreement with the redox-modified peptide pool baited in mouse macrophages by Su *et al.* upon treatment with exogenous oxidants.[43]

Since our aim was to identify a consistent peptide panel reliable to distinguish redox-modified proteins between resting and amyloid activated microglia, we considered only peptides uniquely assigned by proteomics to one protein and identified in at least one technical replica of all the three biological replicates of the microglial cultures used. These stringent comparison criteria yielded 287 peptides out of the 1129 identified. These peptides allowed a confident identification of a total of 193 proteins, even by only one reversible redox modified peptide captured as a biotin adduct (Table S1, ESI‡). To assess the biological processes and the protein functions possibly affected by the acquisition of redox modifications on cysteinyl residues in the microglial proteome, these 193 proteins were clustered into protein function (Fig. 3A) and biological processes (Fig. 3B) according to the Ingenuity Pathways Knowledge Base.

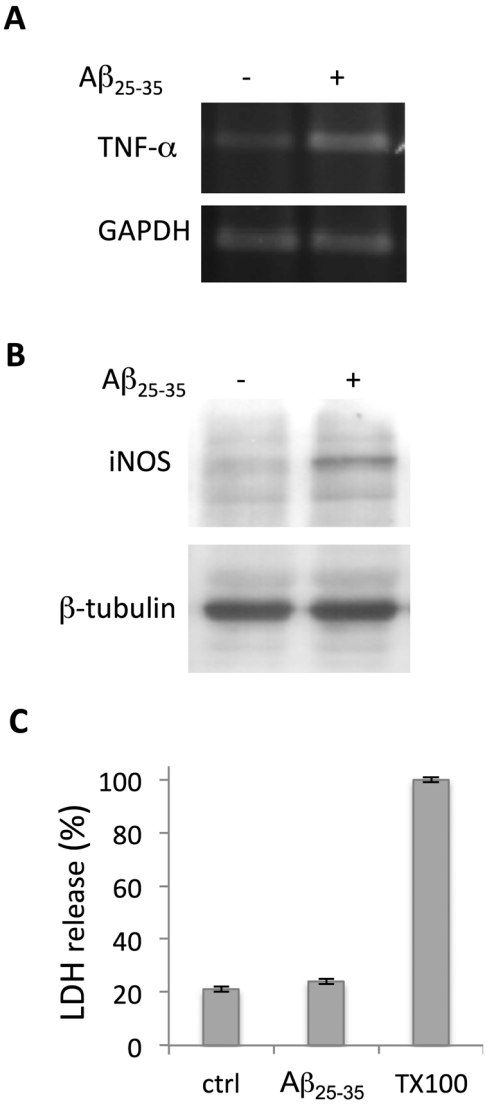

Fig. 2 Effects of $A\beta_{25-35}$ on BV2 cells. (A) Induction of TNF-α in BV2 cells treated for 4 h with 50 μM $A\beta_{25-35}$; TNF-α mRNA was detected by RT-PCR in $A\beta_{25-35}$ untreated (−) and treated (+) cells. The mRNA for GAPDH was used as a reference. (B) Detection of the cytokine-inducible isoform of the nitric oxide synthase (iNOS) in BV2 cells treated for 24 h with 50 μM $A\beta_{25-35}$; iNOS was immunodetected in $A\beta_{25-35}$ untreated (−) and treated (+) cells. β-Tubulin was used as a reference. (C) Cell viability in BV2 treated for 24 h with 50 μM $A\beta_{25-35}$; viability was assessed by measuring LDH released in the culture medium. The values are expressed as a percentage with respect to those obtained by lysing cells with detergent 2% Triton X-100. Ctrl, $A\beta_{25-35}$ untreated cell; $A\beta_{25-35}$, 50 μM $A\beta_{25-35}$ treated; TX100, cells lysed by treatment with Triton X-100.

A detailed analysis of redox modified peptides consistently captured by the biotin–streptavidin approach showed that for a large number of them (223 out of 287, 78%) beta amyloid activation does not induce a change in the redox state. On the other hand, upon treatment with the $A\beta_{25-35}$ peptide we observed a selective enrichment of 40 peptides and a selective missing of 24 redox modified peptides captured in the resting status (Table S2, ESI‡). Indeed, according to the consistent shotgun proteomic identification we obtained, the beta amyloid treatment can induce selective gain or loss of reversible redox modifications on targeted cysteinyl residues for 36 and 21 proteins, respectively, (Table S2, ESI‡). Moreover, an opposite pattern of oxidation for a couple of cysteines of the same protein could be observed for the beta 2-like-1 subunit of the guanine nucleotide-binding protein (RACK1) and for the heterogeneous nuclear proteins K and L (hnRNPK and hnRNPL). In these couple of residues for each of these three proteins, the former cysteinyl residue found to be redox modified in the resting cells lost the modification in the activated ones, whereas the latter cysteinyl gained the modification only in the activated form.

With the aim of validating the changes in the redox profiles we highlighted between resting and activated microglial cells, we ruled out the possibility that different protein expression levels between treated and untreated cells may affect our results. Particularly, we focused on three proteins possibly linking oxidative stress with microglial neurotoxic activity, namely peroxiredoxin-6 (Prdx6), Ras-related C3 botulinum toxin substrate 1 (Rac1) and chloride intracellular channel protein 1 (CLIC1). By immunostaining we proved that the expression level of these three proteins did not change between resting and activated microglia, confirming that their redox modified variants appeared only in the proteome of $A\beta_{25-35}$ stimulated microglia (Fig. 4).

Discussion

The increasing interest in determining post-translational modifications as molecular switches towards alternative protein functions has recently encountered the investigation of the role of oxidative stress in chronic pathologies. In studies focused on redox-modifications of proteins, nitrosylation and glutathionylation have gained a place of honour.[16,18,25]

In this paper, we investigated changes that accompany beta amyloid exposure in the redox landscape of microglia. To approach this issue, we took advantage of a fast and highly selective methodology, based on the biotin–streptavidin affinity system, and combined with MS-based proteomics. In particular, this platform was targeted to specifically isolate reversible redox-modified peptides and thus allowed us to determine the precise cysteinyl residue whose redox states are modulated in the microglial proteome by oxidative stress.

Recent papers suggested that a limited (hundreds) but selective number of proteins are subjected to RRMs.[16] The results reported herein show that considering both the microglia states we addressed, the number of proteins found to be reversible redox modified (193) is in the same range as observed in other cellular models (see references in Table S2, ESI‡).[65–70] As evident from Fig. 3, our data indicate that in microglia RRMs target mainly proteome components involved in protein biosynthesis, which clustered ribosomal proteins, translational regulators and molecular chaperons, and in two other processes, *i.e.* cellular growth/proliferation and inflammation, on which peculiarly the microglial biology is based.[12]

The differential analysis between resting and beta-amyloid activated microglia we provided herein allowed us to identify

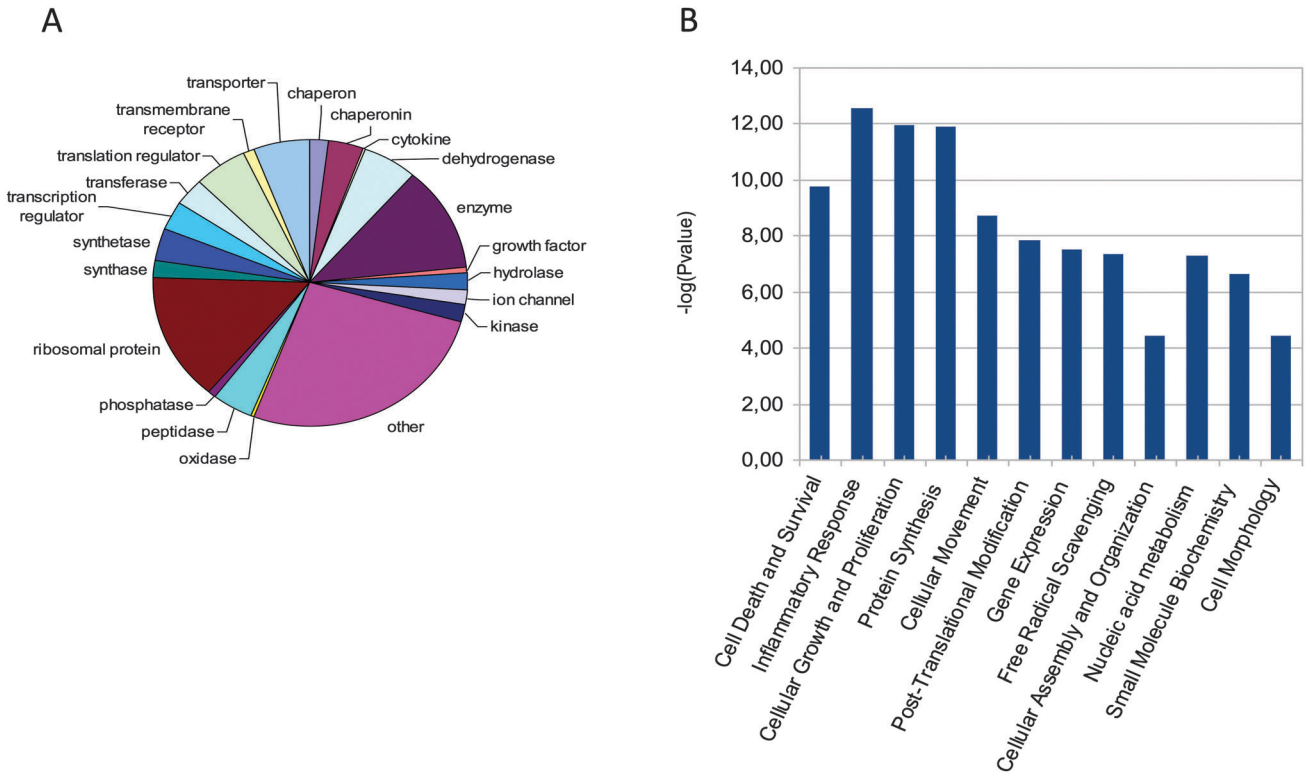

Fig. 3 Analysis of proteins found reversibly redox modified in BV2 cells. Microglial proteome components found to be redox modified on cysteinyl residues were clustered for function (Panel A) and biological processes (Panel B), respectively, according to the Ingenuity Pathways Knowledge Base (IPA). The enrichment of selected biological processes has been evaluated using the IPA algorithm through Fisher's exact test, and reported in panel B as $-\log(p \text{ value})$.

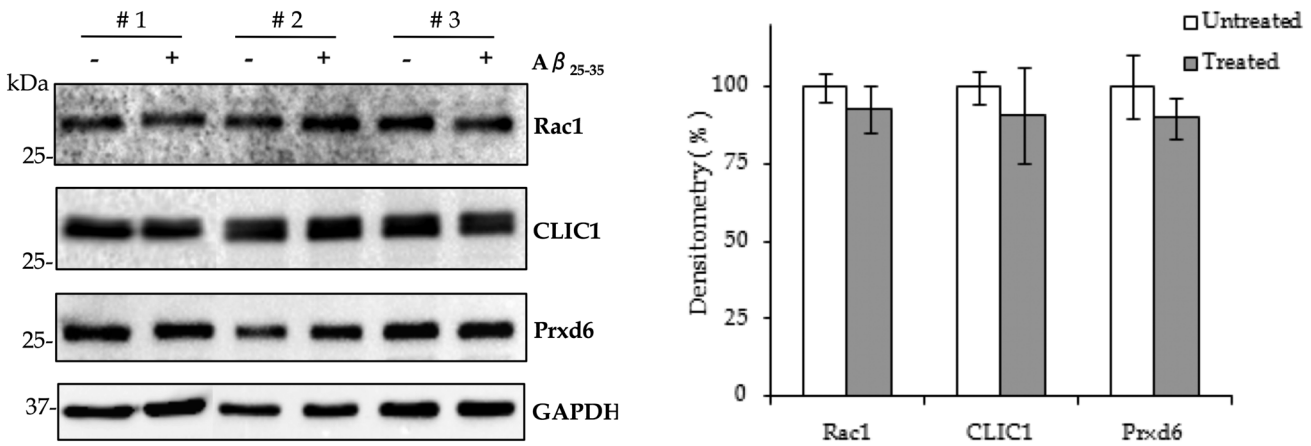

Fig. 4 Expression levels of selected redox modified proteins. On the left, immunodetection of Rac1, CLIC1 and Prdx6 in $A\beta_{25-35}$ treated (+) and untreated (−) cells. All the three independent cell preparations are reported. On the right, relative intensities of the optical densities of each of the three protein bands and the corresponding GAPDH band. Quantitative data are expressed as a percentage with respect to the ratio value determined in the untreated cells. Data were collected from independent cell preparations (n = 3), and averaged (±SD). Statistical analysis was performed by Student's t-test. The p-value of <0.01 was considered statistically significant.

60 proteins in which the redox state of the sensitive cysteinyl site(s) is consistently changed in the activated phenotype (Table S2, ESI‡). Although some of these cysteinyl site(s) have been recently observed as reversible redox modified in other cell models (see references in Table S2, ESI‡), a consistent number of them is novel, and possibly peculiar to the neurotoxic phenotype of microglia we achieved by our experimental setup. Accordingly, we may propose the corresponding proteins as potential redox-based biomarkers of the microglia activated by beta amyloid, to be further validated by structural and functional studies *in vivo*.

Among the proteins selectively redox modified, three proteins were considered, namely peroxiredoxin-6 (Prdx6), Ras-related C3 botulinum toxin substrate 1 (Rac1) and chloride intracellular

channel protein 1 (CLIC1), each of them representative of a link between oxidative stress and microglial neurotoxic activity.

In the case of Prdx6, the cysteine residue we detected (Cys47) is indeed known to be involved in the active site as a free thiol, and forming a transient adduct with the GSH during the enzyme turnover.[44] The selective enrichment of the peptide encompassing the Cys47 residue only in the activated microglia proved that in amyloid injury the reversible redox modified form of the active cysteine is prevalent, and thus under these conditions Prdx6 enhances its catalytic turnover. According to this scenario, Prdx6 should be considered an actor with a protective role against the oxidative stress in microglia, cooperating to sustain the transition toward a chronic neuroinflammatory phenotype and reinforce the role of this protein in AD. Indeed, the participation of Prdx6 in AD has been recently proposed by two different groups in neuronal cell cultures and transgenic mice, although opposite effects of its over-expression have been observed.[45,46]

The other interesting protein of the microglial redox proteome is Rac1, a small GTPase belonging to the Rho GTPase family, which in its active form can bind different protein effectors related to secretory pathways, phagocytosis and apoptosis.[47] Rac1 represents, alternatively with the isoform Rac2 and together with p40phox, p47phox and p67phox, the cytosolic regulatory subunit of the NADPH oxidase complex.[48,49] In the resting microglial status, inactive GDP-bound Rac1 is sequestered in the cytosol by a Rho GDP-dissociation inhibitor (RhoGDI); conversely, after microglia activation, Rac1 is activated through GTP binding, which then dissociates from RhoGDI and translocates to the plasma membrane where it contributes to NADPH oxidase activation.[50] We found a selective enrichment of RRM of Rac1 on Cys105, already annotated as nitrosylated.[51] The role of RRM in enhancing GTP binding has been reported by *in vitro* studies for the alternative Rac2 isoform,[52] which conversely we found to be redox modified both in treated and in untreated microglial cells (Table S1, ESI‡). Hence, our data confirm that Cys105 is a sensitive site on Rac1 toward oxidative stress, and suggest that, in microglia, redox modified-Rac1 may be related to activation of NADPH oxidase.

Finally, another relevant protein which appears to be differently redox modified in the beta amyloid treated microglia with respect to control is CLIC1, a member of the chloride channel protein family. Proteins belonging to this family are involved in many physiological processes such as cell division, cell cycle and apoptosis, and cell differentiation, and also in pathophysiological processes such as neurodegenerative diseases and different types of cancer (reviewed in ref. 53). Among these proteins CLIC1 has been reported to undergo a ''metamorphic'' transition from a soluble form to an integral membrane form upon oxidative stress.[54,55] Once into the plasma membrane, CLIC1 can oligomerize, forming an ion channel for the influx of chloride ions altering the membrane ionic conductance.[56,57] Treatment of microglial cells with amyloid induces their localization on the plasma membrane, and CLIC1 silencing alters both the release of TNF-α and •NO production.[56] Moreover, blockage of CLIC1 stimulates amyloid phagocytosis in mononuclear phagocytes.[58] Recently, it has been proposed that CLIC1 could modify macrophage activity through the modulation of phagosomal acidification.[59] Structural studies on CLIC1 reported that incubation with hydrogen peroxide leads to the formation of an intramolecular disulfide bridge between Cys24 and Cys59, triggering a conformational transition toward a dimer with the ability to colonize a lipid bilayer.[55,60,61] In our analysis, we actually identified peptides encompassing Cys24 by shotgun proteomics of the peptide mixture enriched by a biotin switch only upon amyloid stimulation, but with a very low level of reproducibility among the biological and technical replica we independently processed by shotgun proteomics (data not shown). Conversely, the enrichment of the peptide encompassing Cys191 we observed in activated microglia strongly suggests a possible novel role for this site in the transition of CLIC1 toward the acquisition of the dimeric structure. Interestingly, in a very recent and robust screening of *S*-nitrosylation sites on the human proteome, the same cysteinyl residue has been found to be modified.[62] These data reinforce our hypothesis on the role of Cys191 in the peculiar functions of the highly structurally conserved CLIC1 proteins, in which 98.3% residues out of 241 overlapping are identical between humans and mouse.

Conclusion

An effort has been made to decipher rules of thiol-based switches in a genome-wide manner.[62–64] The ''biotin switch'' and the shotgun proteomics we applied in this study yielded a consistent list of peptide sequences encompassing cysteinyl residues that we pinpointed as sensitive toward redox modifications. The list here reported will provide reliable data for bioinformatics to better refine the knowledge of the physico-chemical features that in proteins constitute the consensus motif for RRMs.

Through this site-specific proteomics approach employed, we were able to successfully infer reversible redox post-translational modifications on target proteins possibly involved in the microglial neuroinflammation phenotype. In our previous studies, we highlighted by expression proteomics that only one protein was up-regulated and a few proteins were down-regulated after $A\beta_{25-35}$ treatment.[11] Here, we observed that a few but critical cellular processes are targeted by RRM modification induced by the amyloid treatment. Taken together, these two studies suggest that the activation of microglia by amyloid is based more on redox post-translational modification activity, fast and selective, rather than on transcriptional modulation. Moreover, for at least two of the proteins identified in this paper, namely Prdx6 and Rac1, we were able to suggest mechanisms through which RRM could affect the peculiar role of microglia in amyloidogenic injury, which at the same time reinforce the oxidative burst and resist toward it. Furthermore, the RRM modulation we observed on CLIC1 reinforces the structural and functional relationship between oxidative stress and its metamorphic transition from a soluble form to an integral membrane form.

In our survey, novel RRM protein targets emerged with respect to those already identified in the neuronal compartment. A deeper

analysis of the involvement of these proteins in microglia activation could disclose further the relationship between the oxidative stress and the molecular basis of cell functions and dysfunctions in the neural tissue.

Acknowledgements

This work was partly supported by an Italian grant from MIUR (to MES; grant number PRIN 2010HEBBB8_002) and a grant from Sapienza University (to MES; grant number C26A124WCR). The funders had no role in study design, data collection and analysis, decision to publish, or preparation of the manuscript. None of the authors have competing interests to declare.

References

1 M. Goedert and M. G. Spillantini, *Science*, 2006, **314**, 777–781.
2 C. Ballard, S. Gautheier, A. Corbett, C. Brayne, D. Aarsland and E. Jones, *Lancet*, 2011, **377**, 1019–1031.
3 C. Haass and D. J. Selkoe, *Nat. Rev. Mol. Cell Biol.*, 2007, **8**, 101–112.
4 R. Rodrigues, R. B. Petersen and G. Perry, *Cell. Mol. Neurobiol.*, 2014, **34**, 925–949.
5 H. L. Hsieh and C. M. Yang, *BioMed Res. Int.*, 2013, **2013**, 484613.
6 V. H. Perry and C. Holmes, *Nat. Rev. Neurol.*, 2014, **10**, 217–224.
7 H. M. Gao, H. Zhou and J. S. Hong, *Trends Pharmacol. Sci.*, 2012, **33**, 295–303.
8 H. Kettenmann, U. K. Hanisch, M. Noda and A. Verkhratsky, *Physiol. Rev.*, 2011, **91**, 461–553.
9 M. K. Jha, J. H. Kim and K. Suk, *Proteomics*, 2014, **14**, 378–398.
10 D. P. Schafer, E. K. Lehrman and B. Stevens, *Glia*, 2013, **61**, 24–36.
11 L. Di Francesco, V. Correani, C. Fabrizi, L. Fumagalli, M. Mazzanti, B. Maras and M. E. Schininà, *Proteomics*, 2012, **12**, 124–134.
12 J. Gimeno-Baygon, A. Lapez-Lapez, M. J. Rodraguez and N. Mahy, *J. Neurosci. Res.*, 2014, **92**, 723–731.
13 R. Requejo, T. R. Hurd, N. J. Costa and M. P. Murphy, *FEBS J.*, 2010, **277**, 1465–1480.
14 B. Groitl and U. Jakob, *Biochim. Biophys. Acta*, 2014, **1844**, 1335–1343.
15 T. Nakamura, D. H. Cho and S. A. Lipton, *Exp. Neurol.*, 2012, **238**, 12–21.
16 C. L. Grek, J. Zhang, Y. Manevich, D. M. Townsend and K. D. Tew, *J. Biol. Chem.*, 2013, **288**, 26497–26504.
17 I. Dalle-Donne, R. Rossi, G. Colombo, D. Giustarini and A. Milzani, *Trends Biochem. Sci.*, 2009, **34**, 85–96.
18 J. J. Mieyal, M. M. Gallogly, S. Qanungo, E. A. Sabens and M. D. Shelton, *Antioxid. Redox Signaling*, 2008, **10**, 1941–1988.
19 E. A. Sabens Liedhegner, X. H. Gao and J. J. Mieyal, *Antioxid. Redox Signaling*, 2012, **16**, 543–566.
20 T. Nakamura, S. Tu, M. W. Akhtar, C. R. Sunico, S. Okamoto and S. A. Lipton, *Neuron*, 2013, **78**, 596–614.
21 S. F. Newman, R. Sultana, M. Perluigi, R. Coccia, J. Cai, W. M. Pierce, J. B. Klein, D. M. Turner and D. A. Butterfield, *J. Neurosci. Res.*, 2007, **85**, 1506–1514.
22 C. Zhang, C. C. Kuo, A. W. Chiu and J. Feng, *J. Alzheimer's Dis.*, 2012, **30**, 919–934.
23 Q. F. Zhao, J. T. Yu and L. Tan, *Mol. Neurobiol.*, 2015, **51**, 268–280.
24 Y. M. Go and D. P. Jones, *J. Biol. Chem.*, 2013, **288**, 26512–26520.
25 B. McDonagh, S. Ogueta, G. Lasarte, C. A. Padilla and J. A. Bárcena, *J. Proteomics*, 2009, **72**, 677–689.
26 E. Blasi, R. Barluzzi, V. Bocchini, R. Mazzolla and F. Bistoni, *J. Neuroimmunol.*, 1990, **27**, 229–237.
27 L. Millucci, R. Raggiaschi, D. Franceschini, G. Terstappen and A. Santucci, *J. Biosci.*, 2009, **34**, 293–303.
28 J. Rappsilber, M. Mann and Y. Ishihama, *Nat. Protoc.*, 2007, **2**, 1896–1906.
29 J. Cox and M. Mann, *Nat. Biotechnol.*, 2008, **26**, 1367–1372.
30 K. Mann and M. Mann, *Proteome Sci.*, 2011, **9**, 7.
31 G. Mermelekas, M. Makridakis, T. Koeck and A. Vlahou, *Expert Rev. Proteomics*, 2013, **10**, 537–549.
32 S. E. Leonard and K. S. Carroll, *Curr. Opin. Chem. Biol.*, 2011, **15**, 88–102.
33 S. Ratnayake, I. H. Dias, E. Lattman and H. R. Griffiths, *J. Proteomics*, 2013, **92**, 160–170.
34 J. Guo, M. J. Gaffrey, D. Su, T. Liu, D. G. Camp, 2nd, R. D. Smith and W. J. Qian, *Nat. Protoc.*, 2014, **9**, 64–75.
35 M. Zaccarin, M. Falda, A. Roveri, V. Bosello-Travain, L. Bordin, M. Maiorino, F. Ursini and S. Toppo, *Free Radical Biol. Med.*, 2014, **71**, 90–98.
36 A. Henn, S. Lund, M. Hedtjarn, A. Schrattenholz, P. Porzgen and M. Leist, *Altex*, 2009, **26**, 83–94.
37 D. Han, S. Moon, Y. Kim, J. Kim, J. Jin and Y. Kim, *Proteomics*, 2013, **13**, 2984–2988.
38 S. Varadarajan, J. Kanski, M. Aksenova, C. Lauderback and D. A. Butterfield, *J. Am. Chem. Soc.*, 2001, **123**, 5625–5631.
39 S. Martire, A. Fuso, D. Rotili, I. Tempera, C. Giordano, I. De Zottis, A. Muzi, P. Vernole, G. Graziani, E. Lococo, M. Faraldi, B. Maras, S. Scarpa, L. Mosca and M. D'Erme, *PLoS One*, 2013, **8**, e72169.
40 V. K. Sonkar, P. P. Kulkarni and D. Dash, *FASEB J.*, 2014, **28**, 1819–1829.
41 R. Ghasemi, A. Zarifkar, K. Rastegar, N. Maghsoudi and M. Moosavi, *Eur. J. Pharmacol.*, 2014, **726C**, 33–40.
42 A. Khan, K. Vaibhav, H. Javed, R. Tabassum, M. E. Ahmed, M. M. Khan, M. B. Khan, P. Shrivastava, F. Islam, M. S. Siddiqui, M. M. Safhi and F. Islam, *Neurochem. Res.*, 2014, **39**, 344–352.
43 D. Su, M. J. Gaffrey, J. Guo, K. E. Hatchell, R. K. Chu, T. R. Clauss, J. T. Aldrich, S. Wu, S. Purvine, D. G. Camp, R. D. Smith, B. D. Thrall and W. J. Qian, *Free Radical Biol. Med.*, 2014, **67**, 460–470.
44 Y. Manevich, S. I. Feinstein and A. B. Fisher, *Proc. Natl. Acad. Sci. U. S. A.*, 2004, **101**, 3780–3785.

45 I. K. Kim, K. J. Lee, S. Rhee, S. B. Seo and J. H. Pak, *Free Radical Res.*, 2013, **47**, 836–846.
46 H. M. Yun, P. Jin, J. Y. Han, M. S. Lee, S. B. Han, K. W. Oh, S. H. Hong, E. Y. Jung and J. T. Hong, *Mol. Neurobiol.*, 2013, **48**, 941–951.
47 T. R. Stankiewicz and D. A. Linseman, *Front. Cell. Neurosci.*, 2014, **8**, 314.
48 N. D'Ambrosi, S. Rossi, V. Gerbino and M. Cozzolino, *Front. Cell. Neurosci.*, 2014, **8**, 279.
49 B. M. Babior, *Blood*, 1999, **93**, 1464–1476.
50 B. L. Wilkinson and G. E. Landreth, *J. Neuroinflammation*, 2006, **3**, 30.
51 Y. J. Chen, W. C. Ku, P. Y. Lin, H. C. Chou, K. H. Khoo and Y. J. Chen, *J. Proteome Res.*, 2010, **9**, 6417–6439.
52 I. S. Kil, S. W. Shin and J. W. Park, *Biochem. Biophys. Res. Commun.*, 2012, **425**, 892–896.
53 H. Singh, *FEBS Lett.*, 2010, **584**, 2112–2121.
54 D. R. Littler, S. J. Harrop, S.-C. Goodchild, J. M. Phang, A. V. Mynott, L. Jiang, S. M. Valenzuela, M. Mazzanti, L. J. Brown, S. N. Breit and P. M. G. Curmi, *FEBS Lett.*, 2010, **584**, 2093–2101.
55 D. R. Littler, S. J. Harrop, W. D. Fairlie, L. J. Brown, G. J. Pankhurst, S. Pankhurst, M. Z. DeMaere, T. J. Campbell, A. R. Bauskin, R. Tonini, M. Mazzanti, S. N. Breit and P. M. Curmi, *J. Biol. Chem.*, 2004, **279**, 9298–9305.
56 G. Novarino, C. Fabrizi, R. Tonini, M. A. Denti, F. Malchiodi-Albedi, G. M. Lauro, B. Sacchetti, S. Paradisi, A. Ferroni, P. M. Curmi, S. N. Breit and M. Mazzanti, *J. Neurosci.*, 2004, **24**, 5322–5330.
57 B. M. Tulk, S. Kapadia and J. C. Edwards, *Am. J. Physiol.: Cell Physiol.*, 2002, **282**, C1103–C1112.
58 S. Paradisi, A. Matteucci, C. Fabrizi, M. A. Denti, R. Abeti, S. N. Breit, F. Malchiodi-Albedi and M. Mazzanti, *J. Neurosci. Res.*, 2008, **86**, 2488–2498.
59 L. Jiang, K. Salao, H. Li, J. M. Rybicka, R. M. Yates, X. W. Luo, X. X. Shi, T. Kuffner, V. W. Tsai, Y. Husaini, L. Wu, D. A. Brown, T. Grewal, L. J. Brown, P. M. Curmi and S. N. Breit, *J. Cell Sci.*, 2012, **125**, 5479–5488.
60 S. C. Goodchild, M. W. Howell, N. M. Cordina, D. R. Littler, S. N. Breit, P. M. Curmi and L. J. Brown, *Eur. Biophys. J. Biophys. Lett.*, 2009, **39**, 129–138.
61 S. C. Goodchild, M. W. Howell, D. R. Littler, R. A. Mandyam, K. L. Sale, M. Mazzanti, S. N. Breit, P. M. Curmi and L. J. Brown, *Biochemistry*, 2010, **49**, 5278–5289.
62 Y. I. Lee, D. Giovinazzo, H. C. Kang, Y. Lee, J. S. Jeong, P. T. Doulias, Z. Xie, J. Hu, M. Ghasemi, H. Ischiropoulos, J. Qian, H. Zhu, S. Blackshaw, V. L. Dawson and T. M. Dawson, *Mol. Cell. Proteomics*, 2014, **13**, 63–72.
63 C. Sun, Z. Z. Shi, X. Zhou, L. Chen and X. M. Zhao, *PLoS One*, 2013, **8**, e55512.
64 Y. J. Chen, C. T. Lu, T. Y. Lee and Y. J. Chen, *Bioinformatics*, 2014, btu301.
65 M. Liu, J. Hou, L. Huang, X. Huang, T. H. Heibeck, R. Zhao, L. Pasa-Tolic, R. D. Smith, Y. Li, K. Fu, Z. Zhang, S. H. Hinrichs and S. J. Ding, *Anal. Chem.*, 2010, **82**, 7160–7168.
66 J. S. Paige, G. Xu, B. Stancevic and S. R. Jaffrey, *Chem. Biol.*, 2008, **15**, 1307–1316.
67 H. Ye, B. Li, V. Subramanian, B. H. Choi, Y. Liang, A. Harikishore, G. Chakraborty, K. Baek and H. S. Yoon, *Biochim. Biophys. Acta*, 2013, **1828**, 1083–1093.
68 R. Scheving, I. Wittig, H. Heide, B. Albuquerque, M. Steger, U. Brandt and I. Tegeder, *J. Proteomics*, 2012, **75**, 3987–4004.
69 Y. W. Lam, Y. Yuan, J. Isaac, C. V. Babu, J. Meller and S. M. Ho, *PLoS One*, 2010, **5**, e9075.
70 D. Tello, C. Tarín, P. Ahicart, R. Bretón-Romero, S. Lamas and A. Martínez-Ruiz, *Proteomics*, 2009, **9**, 5359–5370.

